

Theoretical Transmission Spectra During Extrasolar Giant Planet Transits

S. Seager¹, D. D. Sasselov^{2,3}

ABSTRACT

The recent transit observation of HD 209458 b — an extrasolar planet orbiting a sun-like star — confirmed that it is a gas giant and determined that its orbital inclination is 85° . This inclination makes possible investigations of the planet atmosphere. In this Letter we discuss the planet transmission spectra during a transit. The basic tenet of the method is that the planet atmosphere absorption features will be superimposed on the stellar flux as the stellar flux passes through the planet atmosphere above the limb. The ratio of the planet's transparent atmosphere area to the star area is small ($\sim 10^{-4}$); for this method to work very strong planet spectral features are necessary. We use our models of close-in extrasolar giant planets to estimate promising absorption signatures: the alkali metal lines, in particular the Na I and K I resonance doublets, and the He I $2^3S - 2^3P$ triplet line at 1083.0 nm. If successful, observations will constrain the line-of-sight temperature, pressure, and density. The most important point is that observations will constrain the cloud depth, which in turn will distinguish between different atmosphere models. We also discuss the potential of this method for EGPs at different orbital distances and orbiting non-solar-type stars.

Subject headings: planetary systems — radiative transfer — stars: atmospheres

1. Introduction

The recent transit detection of HD 209458 b (Charbonneau et al. 1999a; Henry et al. 1999) concludes a period of eager anticipation since the first close-in extrasolar giant planet (CEGP), 51 Peg b, was discovered in 1995 (Mayor & Queloz 1995). Five close-in extrasolar giant planets with radii ≤ 0.05 AU are known, and there are an additional six closer than 0.15 AU (see e.g. Schneider 1999). The chance of a transit for a CEGP — assuming random alignment of the orbital inclination — is roughly 10%. Transits have been excluded for five of the 11 above planets (Henry et al. 1999, 1997; Baliunas et al. 1997; Henry, private communication.) The transit of HD 209458 b confirms that the CEGPs are gas giants, gives the planet radius, and fixes the orbital inclination, which removes the *sini* ambiguity in mass and provides the average planet density.

While the transit gives important planet parameters, it cannot provide any information about the planet atmosphere. Nevertheless, the edge-on orbital inclination means that HD 209458 b is promising for a number of different planet atmosphere investigations. One is the transit transmission spectra discussed in this Letter. Other methods benefit from an edge-on system because a near full planet phase will occur, providing the maximum amount of reflected light. A second method is a spectral separation technique

¹School of Natural Sciences, Institute for Advanced Study, Olden Lane, Princeton, NJ, 08540

²Astronomy Department, Harvard University, 60 Garden St., Cambridge, MA, 02138

³Alfred P. Sloan Research Fellow

that searches the combined star-planet flux for the reflected spectrum of the planet, assuming that the planet reflects the stellar features exactly in a small wavelength region and using the Doppler shift of the planet spectrum. Cameron et al. (1999) claim a possible detection of reflected light from τ Boo b at an inclination of 29° and with a planet-star flux ratio of 1.9×10^{-4} . Charbonneau et al. (1999b) claim a null detection on the same system, using the same technique and give an upper limit of a flux ratio of 5×10^{-5} for inclinations near 90° and 1.1×10^{-4} for $i = 29^\circ$. The observed flux ratio gives a product of the albedo and square of planet radius, given the known planet-star distance. With an assumption of planet radius (R_P), the albedo would weakly constrain the type and size distribution of condensates in the planetary atmosphere. A third atmosphere observation method is described by Seager, Whitney, & Sasselov (1999), by theoretical investigations of optical light curves and polarization curves of the CEGP systems as the planet reflects stellar light at different planet phases. Light curve observations — which range from a few to 100 μ mag depending on the planet radius and the cloud type — have maximum amplitude for high inclinations, especially for grains which have a large backscattering probability in a narrow angular range. Planned observations of CEGPs in thermal emission in the infrared with, for example, the Keck infrared interferometer in differential phase mode, will not depend on a favourable orbital inclination.

A fundamental question about the CEGPs is whether or not they are bright in reflected light. Because of their proximity to the central star the CEGPs could at best be as bright as four orders of magnitude fainter than their parent star, compared to Jupiter which is ten orders of magnitude fainter than the Sun. However, Seager et al. (1999) show that the optical albedo depends highly on the type and size distribution of condensates in the atmosphere, condensate heating, and cloud assumptions. Sudarsky, Burrows, & Pinto (1999) show that with clouds located at the 10 bar level and 1 pressure scale height high, and using ad hoc modified T-P profiles to simulate heating of the CEGP, alkali metal absorption will dominate in the optical redward of 500 nm, resulting in dark CEGPs. The issue of the albedo is not relevant to transmission spectra, but as discussed in this Letter cloud depth is.

The idea of spectral transmission observations is not new: they have been observed in binary stars (e.g. Eaton 1993); they have been extensively observed and analyzed for Solar System planet stellar and Solar occultations (e.g. Smith & Hunten 1990); they are one motivation for large transit surveys of stars with no known CEGPs (e.g. Vulcan Camera Project (PI W. Borucki), STARE (PI T. Brown), WASP (PI S. Howell)); they have been discussed briefly for extrasolar planets (e.g. Schneider 1994; Charbonneau et al. 1999a); and they have been discussed for extrasolar planet exospheres. Here, for the first time to our knowledge, we quantify the method for CEGPs and provide estimates of specific spectral features in the combined star-planet light during a planet transit. Many more CEGPs will be detected in the near future both by ongoing radial velocity searches and by wide-field transit searches. The transit transmission lines will provide us with constraints on cloud-top depth, and column density, temperature (T), and pressure (P) along the line-of-sight through the planet's transparent atmosphere.

2. Transmission Spectra

During an EGP planetary transit, the planet passes in front of the star and occults the stellar flux in the amount equal to the ratio of the planet to star area. During the transit, some of the stellar flux will pass through the optically thin part of the planet atmosphere, the part of the atmosphere above the planet limb. Here we define the planet limb as the boundary (e.g. the cloud tops) above which the planet's atmosphere is transparent to the stellar continuum radiation. We call the entire atmosphere above the limb the “transparent atmosphere”, although the transparent atmosphere is optically thick in some transitions.

Below the limb the optically thick clouds prevent radiation from being transmitted through the atmosphere. The ratio of the planet's projected transparent atmosphere area to star-minus-planet area is small, on the order of 10^{-4} , using $R_* = 1.3R_\odot$, $R_P = 1.54R_J$ (based on HD 209458 parameters from Mazeh et al. 1999), and using an estimate for the limb radial depth of $0.005 R_P$. The planet's absorption features will be superimposed on the observable stellar flux, and will appear at the $\sim 10^{-4}$ level below the continuum flux. Very strong spectral features are needed for detection; essentially the absorption features must be optically thick. In contrast to reflected planetary light, the transit transmission flux is not diluted by the planet-star distance, and is not cloud albedo-dependent.

During Solar System planet transit occultations and binary star occultations successive measurements are made as the planet occults the star (i.e. during ingress or egress). The time-dependent change in spectral features provide column density and temperatures for different atmosphere heights. Because the CEGP is much smaller and fainter than the parent star this will not be possible in the near future. The best orbital phase for the transmission spectra observations of CEGPs is when the planet is fully projected on the visible hemisphere of the star so that the planet's projected transparent atmosphere takes out the greatest area and limb darkening from the star has no effect.

In stellar occultations by planets in the Solar System, the limb of giant planets is usually defined at (1) the cloud tops, or (2) at the 1-bar level (Atreya 1986). Here we define the limb at the cloud tops, where the clouds are taken to be 1 pressure scale height above the cloud base, which due to irradiation heating is expected to be well above the 1 bar level.

Refraction through the CEGP's atmosphere has to be accounted for in defining the limb and in computing the total optical path of rays reaching us through it. During the solar transit of Venus in 1761 an obvious refraction effect at second contact convinced Lomonosov in St. Petersburg that Venus had an atmosphere (Cruikshank 1983). However, the cloud tops in our model of HD 209458 b (see below) are high in its atmosphere, where the gas density is fairly low and refraction is small. In an isothermal atmosphere with gas scale height H , the angle of refraction for a ray passing at planetocentric distance r is: $\theta = \nu(r)[(2\pi R_P)/H]^{1/2}$, where $\nu(r) = n - 1$ is the atmospheric refractivity at r (for a $H_2 + He$ mixture: $\sim 1.2 \times 10^{-4}$), with $n(\lambda, r)$ the index of refraction. Refraction introduces a lengthening of the pathways of the rays through a spherical plane-parallel stratified atmosphere: $\Delta s = 0.5z\theta^2$, where simply $z^2 = (R_P + H)^2 - R_P^2$. Unlike stellar occultations by our Solar System planets, for CEGP transits the parent star is an extended background source and subtends a significant solid angle at its orbit. However, for cloud tops in HD 209458 b at $P < 10^4 \text{ dyn cm}^{-2}$, $\Delta s < 2\%$.

2.1. Close-in EGPs Transparent Atmosphere Model

We consider the only currently known EGP system with an observed transit, HD 209458. We use the stellar parameters $R_* = 1.3R_\odot$, $T_{\text{eff}} = 6000$, $\log g = 4.25$, and $[\text{Fe}/\text{H}] = 0.0$, derived from evolutionary calculations and fits to spectroscopic data in Mazeh et al. (1999). We use the planetary parameters $R_P = 1.54 R_J$, $M_P = 0.69 M_J$, $\log g = 2.9$, and $i = 85.2^\circ$ derived from the transit observations and radial velocity observations, together with the stellar parameters (Mazeh et al. 1999). For a circular orbit we derive a semimajor axis $a = 0.0468 \text{ AU}$. We compute the incident flux of HD 209458 with the above parameters from the model grids of Kurucz (1992).

We compute the CEGP atmosphere (temperature-pressure (T-P) profile and emergent spectra) using our code described in Seager (1999) and Seager et al. (1999). This code is improved over the version

described in Seager & Sasselov (1998) in two major ways. One is a Gibbs free energy minimization code to calculate solids and gases in chemical equilibrium, the second is condensate opacities for 3 solid species. So while in Seager & Sasselov (1998) we considered neither the depletion of TiO nor formation of MgSiO₃, in the new models we do. One of the largest uncertainties in the atmosphere models is the location of clouds, and the cloud particle type and size. In Seager et al. (1999) we find that the T-P profile and the emergent flux (reflected + thermal) depends entirely on the condensate assumptions.

Because we define the planet limb at the cloud tops, the cloud wavelength-dependent albedos are not directly important. Furthermore, even if the clouds were not optically thick, they would not superimpose any spectral features on the optical stellar flux since their extinction (absorption + scattering) is generally a smooth function of wavelength.

2.1.1. *Transparent Atmosphere Temperature-Pressure Profile*

We use the radial T-P profile generated in the self-consistent irradiated atmosphere code, and construct a limb depth and line-of-sight T-P profile from geometrical considerations. The limb of the planet, defined above, is approximately 0.01 R_P . Together with $R_P = 1.54R_J$ and $R_* = 1.3R_\odot$, the ratio of the projected transparent atmosphere to the stellar disk is 3.6×10^{-4} . The line-of-sight T-P profile describes a plane-parallel column of gas through which the stellar flux passes. The gas is optically thin; flux at most wavelengths passes through relatively unattenuated. We compute the sum through several line-of-sight columns of gas, from the densest column tangential to the cloud top to the column that just skims the uppermost atmosphere. However, in an atmosphere with exponential density fall off, almost all of the absorption occurs in the densest column.

To solve for the radial atmosphere structure we must make a specific assumption about cloud particle type and size. Here we consider 10 μm grains of MgSiO₃, Fe, and Al₂O₃. For this particular model ($T_{\text{eff}} = 1350$ K), the transparent atmosphere above the limb is comprised of a gas between 850-1000 K with pressures 20-600 dyne cm⁻². The main constituents of a gas at these temperatures and pressures are H₂, CO, H₂O, and He. Because of the irradiation heating, CO dominates over CH₄ in this CEGP model. Most gases are in molecular form with the exception of He and the alkali metals. The volatile elements (e.g. Mg, Ca, Ti), have condensed into grains and we assume they have settled to the cloud base. Photochemistry is not included, but the UV radiation from the parent star could photoionize a small fraction of H₂, CO, etc. through the transparent atmosphere. This, however, would have little consequence on the results (See §2.2.3).

2.1.2. *Cloud Models*

We caution that the transmission spectra presented here are estimates that depend on several assumptions. Once observations are successful, a more careful computation to accurately interpret the data is necessary. One point to make is that the location of the cloud base — and hence the cloud tops — depends on the irradiation heating of the planet atmosphere, which itself depends heavily on the type and size of condensates present throughout the planet atmosphere. In this particular model we consider 10 μm grains of MgSiO₃, Fe, and Al₂O₃. While the MgSiO₃ clouds are the highest in the atmosphere, all are important for computing the irradiated T-P profile. The choice of cloud particle type and size distribution is highly uncertain, and the most complex free parameter of the models. In Seager et al. (1999) we discuss

this in more detail.

Another major assumption used is that the radial T-P profiles are similar on all parts of the planet. This would be the case if strong winds redistribute the heat efficiently (e.g. as on Jupiter where there is no apparent difference from one side of the terminator to the other.) A different line-of-sight T-P profile does not change our predictions much; the flux-ratio is set by the planet limb, star area, and planet area, and the features are superimposed on that. Indeed it is very difficult to predict the exact line shape with so many unknowns about the planet atmosphere such as element abundances (from both planet metallicity and non-equilibrium chemistry) and cloud location due to heating.

2.2. Results

The CEGP and parent solar-type star have almost no spectral features in common; at effective temperatures (T_{eff} s) of ~ 1100 K to ~ 1600 K, the CEGPs are almost 5 times cooler than the stars at T_{eff} 's 5000–6000 K. Thus, the transmission spectra method is promising. In this subsection we discuss strong signals in the planetary atmosphere.

2.2.1. Alkali Metals

The Na I and K I resonance doublets are predicted to be strong in CEGPs (Seager et al. 1999; Sudarsky et al. 1999), assuming the atmospheres are similar to brown dwarfs and cool L dwarfs which have similar T_{eff} s. Alkali metals have clear signatures in cool L dwarfs and brown dwarfs where the metals such as Ti have condensed out of molecular form into solids, depleting the strong optical molecular absorbers. The K I doublet $4^2S - 4^2P$ absorption line at 767.0 nm is extremely broad in methane dwarfs, such as Gliese 229B, which have T_{eff} s a few hundred degrees lower than the CEGPs. The broad wings of the K I resonance doublet extend for several tens of nm and are responsible for the large continuum depression in the optical and flux slope redward to 1 μm (Tsuiji et al. 1999; Burrows et al. 1999). The broad lines are caused by strong pressure broadening by H_2 , and are in part so prominent because there are no other strong absorbers present at those wavelengths throughout the entire photosphere. There is some question about the shape of the alkali metal lines in the CEGP atmospheres; they will be very broad if the clouds are low in the photosphere and the large pressures deep in the photosphere can contribute to strong line broadening. Sudarsky et al. predict this scenario where K I and Na I absorb essentially all incoming optical radiation redward of 500 nm. Seager et al. (1999) include heating from the parent star on the T-P profile, and find that the lines are much narrower, since clouds exist higher in the atmosphere at lower pressure. Nevertheless, in the transparent atmosphere of the planet, the K I and Na I resonance lines will be narrow — the deep pressure zones where the broad line wings are formed are not sampled.

With the columns of gas defined above (§2.1.1) we compute the attenuation of the incoming intensity with the radiative transfer equation in the limit of no scattering $I(\nu, z) = I_*(\nu, z)\exp(-\kappa(\nu, z))$, where $I_*(\nu, z)$ is the stellar intensity, ν is the frequency, and z is the depth along the line-of-sight through the planet's transparent atmosphere. Here $\kappa(\nu, z)$ is the extinction which includes absorption and scattering. We include the scattering term as 1/4 of the true scattering to estimate isotropic scattering. Our code includes the dominant opacities expected for cool L dwarfs and brown dwarfs: H_2O , TiO , CH_4 , $\text{H}_2\text{-H}_2$ and $\text{H}_2\text{-He}$ collision induced opacities, Rayleigh scattering from H, He, H_2 , and the alkali metal lines. The oscillator strengths and energy levels of the alkali metals (Na, K, Li, Rb, Cs) were taken from Radzig &

Smirnov (1985) and the Kurucz atomic line list (Kurucz CD ROM 23), and we compute line broadening using a Voigt profile with H_2 and He broadening and Doppler broadening. We do not need to solve the full radiative transfer equation since we assume the effect of transmitted intensity through the planet's transparent atmosphere is negligible with regard to the radiative structure which is already accounted for in the irradiation model.

Figure 1 shows the flux from the star and the stellar flux that has passed through the planet's transparent atmosphere. The curves are essentially the same in the UV through the optical, with the exception of the absorption lines: Na I at 285.4 nm and 342.8 nm, the Na I resonance doublet at 589.4 nm and the K I resonance doublet 767.0 nm. The He I triplet line is at 1083 nm. In the infrared, the stellar flux is absorbed by the water bands, as well as the $5\mu m$ and the $3.3\mu m$ methane band (not visible in the figures). No molecular features such as TiO appear in the spectra, since those molecules have been depleted into solids. Other alkali metal lines such as Cs, Rb, and Li do not appear because their abundance — and hence optical depth — is very small, a few orders of magnitude smaller than K. Solar-type stars also have alkali metal lines but they are weak because most of the alkali metals are ionized. In addition, the stellar optical spectrum is crowded with other atomic absorption lines.

Figure 2 shows the planet-star flux ratio below 1000 nm, i.e. the ratio of the stellar flux transmitted through the planet's transparent atmosphere to the stellar flux. The same lines discussed for Figure 1 are apparent. The fixed ratio of the continuum is the ratio of the projected transparent atmosphere area to the star area. Rayleigh scattering from H_2 is important below 200 nm, otherwise it is negligible. Because the lowest level alkali resonance lines are optically thick at line center, virtually no stellar flux transmits through the planet's transparent atmosphere at the line core. The Na I resonance doublet is broader than the K I resonance doublet because its abundance is an order of magnitude higher. With a width of < 1 nm from H_2 pressure broadening, the K I and Na I lines are not much broader than the stellar alkali metal lines (compared to the model discussed below) which have a width of only ~ 0.3 nm.

Figure 2 also shows the transmission spectra from an atmosphere with a cloud base much deeper than predicted by our model, at 0.2 bar instead of at 2.4×10^{-3} bar. (We note that in our range of models for different condensate type and size the highest clouds have bases ranging from roughly 0.5 to 10^{-3} bar.) There will be two main consequences. First the transparent atmosphere area will be larger, resulting in the planet features being a factor of 2–3 higher with respect to the stellar continuum flux. Second, the stellar flux will pass through higher densities, pressures, and temperatures. Rayleigh scattering is strong in this relatively high density transparent atmosphere. When higher pressures are sampled by the transmitting photons, the lines become more pressure broadened. This is seen in the Na I and K I resonance doublets. The higher densities will cause stronger alkali lines and additional absorption lines from other transitions that were too weak to appear in the low densities of our line-of-sight model, for example, non-resonance lines of Na I and K I and Li, Cs, and Rb lines. Observations of the alkali metal lines will be able to constrain cloud location.

2.2.2. Neutral Helium

We expect a strong absorption line at 1083 nm due to scattering of background stellar photosphere photons off the overpopulated He atoms excited to the triplet 2^3S metastable state. The mechanism works as follows. The stellar EUV radiation shortward of 50.4 nm will photoionize neutral He atoms and they will recombine at the local kinetic temperature, which may be as low as 800 K in the upper atmosphere of the

planet. The He I recombination cascade is efficient for the singlet states, but stops at 2^3S for the triplet states which lack a fast radiative decay path to the ground state. Due to the low local kinetic temperature, collisional de-excitation is negligible. On the other hand, the number of 1083 nm continuum photons from the G0V star is very large – they scatter efficiently in the $2^3S - 2^3P$ transition and produce the strong absorption feature in the transmission spectrum.

Versions of this mechanism are responsible for enhanced He I 1083 nm absorption in solar spectra (Zirin 1975; Andretta & Jones 1997), Algol binary systems (Zirin & Liggett 1982), etc. In the case of HD 209458, a sun-like star, we assume the EUV radiation to be that of the Sun (from Tobiska 1991). We use the T-P distribution of the transparent atmosphere generated in the Seager & Sasselov code and illuminate it with that diluted EUV field, simultaneously solving the NLTE transfer for a helium model atom with singlet and triplet states up to $n = 4$. The details of this calculation are essentially the same as in Sasselov & Lester (1994). One has to realize that this calculation is more of an estimate than an fully consistent treatment of He I 1083 nm line formation in the unusual conditions of the EGP’s atmosphere. However, the mechanism described above is very robust and given no other competing target(s) for the EUV photons except H and H₂, the $2^3S - 2^3P$ transition is optically thick at line center. In fact, He (and H) are prone to creating an extended exosphere around the planet; if so, the strength of the He I 1083.0 nm absorption may well be extremely strong (due to a much larger transparent atmosphere) and easy to observe. The broadening of the line (~ 0.3 nm) is not significant, but this needs further study in terms of He collisional broadening by molecular species like H₂.

In the spectrum of the inactive parent star, the He I 1083.0 nm triplet line is extremely weak, if it is present at all. This makes it a promising signature in the combined planet-star flux. Enhanced absorption of the $3^3P - 3^3D$ transition of C is also seen in binary systems, but in the CEGP atmospheres the C is locked in CO or CH₄.

2.2.3. UV and Infrared Wavelengths

Solar System outer planet occultation transmission lines have been very successfully observed in the UV where the molecules such as H₂, N₂, and O₂ have strong absorption signatures. In addition, in CEGPs the H resonance line transitions are strong (and may be enhanced by photodissociation of H₂) and alkali metal resonance line absorption appears in the near-UV (Figure 2). For the CEGPs orbiting sun-like stars, the UV flux is very low, and the lines will be difficult to detect.

The spectral transmission signatures in the infrared (e.g. H₂O and CH₄) shown in Figures 1 and 3 will be difficult to distinguish from the planet’s own thermal emission, which is present at all phases. More importantly, redward of 2000 nm, the planet’s thermal emission which roughly follows a blackbody (dotted line in Figure 1), will be much stronger than the transmitted spectrum which follows the optical-peaking stellar spectrum. This is in contrast to the optical where the planet has no emission; during transit the optical transmission spectrum is the planet’s only contribution to the total flux. Blueward of 2000 nm the transmission spectrum may be brighter than the planet’s own emission although for some models the planet’s thermal emission can be much higher than a blackbody in that region (Seager 1999). In the 0.2 bar cloud base model (Figure 3) where the stellar flux transmits through higher planet atmosphere densities, there is much more absorption by H₂O and CH₄, making the infrared transmission line detection longward of ~ 1400 nm impossible.

In principle the infrared magnitude of the brightness of the planet will increase slightly just after first

contact as illumination passes through the top of the transparent atmosphere, but against the backdrop of the star this will not be detectable. CO lines (not included in this model) may also be good transmission signatures in the infrared.

2.2.4. Comparison of spectra using different R_P and R_*

We have also run calculations using $R_P = 1.27$ (and $i = 87^\circ$) from Charbonneau et al. (1999a), who assumed $R_* = 1.1$. In this case the ratio of planet-to-star area is slightly lower ($\sim 5\%$) than with the correct values due to the higher inclination. In our self-consistent models, the effect of a smaller planet radius and smaller stellar radius decreases the transmitted-to-stellar flux ratio by an even smaller amount. The reason is that a smaller star and planet means the star-planet distance is larger, making the planet's atmosphere slightly cooler. The cooler atmosphere has the MgSiO_3 cloud-top lower in the atmosphere and hence has a larger transparent atmosphere area compared to the hotter model. For example, the equilibrium effective temperature is $T_{\text{eq}} = T_*(R_*/2D)^{1/2}[(1 - A)]^{1/4}$, where T_* is the effective temperature of the star, and A is the Bond albedo. Because $T_{\text{eq}} \sim R_*^{1/2}$, decreasing R_* from $1.3R_\odot$ to $1.1R_\odot$ will change the planet's T_{eq} by ~ 100 K.

There is also a small change due to density. At the same optical depth, the smaller radius planet with a higher surface gravity will have a higher density compared to the planet with a larger radius. Thus in comparison the absorption lines will be slightly stronger, for the same optical depth.

3. Other EGPs

As of this writing there are 29 known extrasolar planets around 27 stars. $M_{\text{sin} i}$ ranges from 0.42 to $11 M_J$ and planet-star distances from 0.042 AU to 2.5 AU. In principle observations of the transmission features of any transiting planet can be attempted. Many of the stars are being monitored for transits, and transits around several of these stars have been excluded (Henry et al. 1999, 1997; Baliunas et al. 1997). Three others of these known planet systems have their inclinations limited by observation of Kuiper-belt-like disks (Trilling et al. 1999). Wide-field transit searches are excluded to transiting systems and are mostly sensitive to systems with orbital distances below 0.2 AU.

CEGPs much more massive than HD 209458 b will have a much smaller transparent atmosphere area. The planet radius is a weak function of mass (Guillot et al. 1996) and more massive planets are expected to be more compact as the degenerate core increases at the expense of the gaseous atmosphere. For a more massive planet with all other parameters equal (atmosphere structure, radius, etc.), the scale height is smaller, and defined by optical depth the entire atmosphere including the transparent atmosphere is smaller. For example τ Boo b which has $m \sin i = 3.87$ (Butler et al. 1997) is at least 5.6 times more massive than HD 209458 b. CEGPs with higher T_{eff} s than HD 209458 b (e.g. τ Boo b) may have cloud bases closer to the top of the atmosphere, also resulting in a smaller transparent atmosphere area. The flux ratio of transmitted to total stellar flux is also sensitive to the stellar radius, and would change by a factor of three for solar-type parent stars; from evolutionary calculations (Ford, Rasio, & Sills 1999) the solar-type parent stars of known CEGPs with orbital distances below ~ 0.2 AU range from 0.93 – $1.56 R_\odot$.

Wide-field transit searches will find short-period planets orbiting stars where radial velocity planet detections are not possible, for example around active cool stars and hot stars that have rotationally

broadened atomic lines and activity. The parent stars of known EGPs range from F6IV (τ Boo) down to M4V (Gliese 876). Planet transmission spectra may be difficult to disentangle from parent M stars whose optical spectra are very crowded with molecular lines such as TiO and VO. Nevertheless, because of the larger planet-to-star area ratio, the flux ratio is enhanced by a factor of ~ 10 . Jupiter-sized planets orbiting hot stars such as a B or O star would have a flux ratio decreased compared to solar by a factor of 10-100, but the UV flux (observed from space) would provide many useful molecular absorption signatures such as H₂, N₂, and O₂.

4. Summary and Prospects

In this Letter we have estimated the transmission spectra of a CEGP during an occultation of the parent star. We find very strong absorption signatures of Na I and K I, and a strong signature of the He I $2^3S - 2^3P$ triplet line at 1083.0 nm. We find the number, strength, and depth of spectral features are sensitive to the cloud-top depth in the planet atmosphere.

Detecting spectral features will require high resolution, high signal-to-noise observations. During the transit of HD 209458, the Doppler shift of the planet is strong enough so that it should be taken into account when analysing the spectra. In addition spectral separation techniques (e.g. Charbonneau et al. 1999b; Cameron et al., 1999) to search for the spectral lines may help recover the weak planet signal. Systematic red or blue shifting from winds blowing between the day and night side may have a detectable effect on the planet spectrum (T. Brown, private communication). Measurements of metallic lines will also constrain (together with M_P , R_P , and ρ_P) the interior models and shed light on the formation scenario of CEGPs, e.g. core accretion vs. gravitational disk instability. The CEGP's extended exosphere may be easy to detect in the He 1083.0 nm transition.

If successful, observations of transmission spectra will be the first made of an extrasolar planet atmosphere, and will provide constraints on the upper atmosphere column density, temperature, and pressure. In addition the observations should easily constrain the cloud-top depth, which naturally defines the planet limb. This information will help distinguish between atmosphere models. Most importantly, detection of the alkali metal absorption lines will confirm the very basic postulate that the CEGPs have similar atmospheres to methane dwarfs and cool L dwarfs which have similar T_{eff} s.

We are grateful to Dave Latham for providing the stellar and planet parameters for the HD 209458 system before publication. We thank Bob Noyes, Tim Brown and Mark Marley for reading the manuscript and for helpful comments and discussion. We also thank Dave Charbonneau and Avi Loeb for useful discussions. SS is supported by NSF grant PHY-9513835. DDS acknowledges support from the Alfred P. Sloan foundation.

REFERENCES

Andretta, V., & Jones, H. P. 1997, ApJ, 489, 375
 Atreya, S. 1986, *Atmospheres and Ionospheres of the Outer Planets and their Satellites* (New York: Springer Verlag)
 Butler, R. P., Marcy, G. W., Williams, E., Hauser, H., & Shirts, P. 1997, ApJ, 483, 457

Burrows, A., Marley, M., & Sharp, C. 1999, astro-ph/9908078

Cameron, C. C., Horne, K., Penny, A., & James, D. 1999, *Nature*, in press

Cruikshank, D. P., 1983, in *Venus*, eds. Hunten, D., Colin, L., Donahue, T., & Moroz, V., (Tucson: University of Arizona Press), p.1

Baliunas, S. L., Henry, G. W., Donahue, R. A., Fekel, F. C., & Soon, W. H. 1997, *ApJ*, 474, L119

Charbonneau, D., Brown, T., Latham, D., & Mayor, M. 1999a, *ApJL*, in press

Charbonneau, D., Noyes, R. W., Korzennik, S. G., Nisenson, P., Jha, S., Vogt, S. S., & Kibrick, R. 1999b, *ApJ*, 522, L145

Eaton, J. A. 1993, *ApJ*, 404, 305

Ford, E. B., Rasio, F. A., & Sills, A. 1999, *ApJ*, 514, 411

Henry, G., Marcy, G., Butler, P., & Vogt, S. 1999, IAU telegramme 7307

Henry, G. W., Baliunas, S. L., Donahue, R. A., Fekel, F. C., & Soon, W. 1999, submitted to *ApJ*

Henry, G. W., Baliunas, S. L., Donahue, R. A., Soon, W. H., & Saar, S. H. 1997, *ApJ*, 474, 503

Kurucz, R. 1992, in *IAU Symp. 159, Stellar Population of Galaxies*, ed. B. Barbuy & A. Renzini (Dordrecht: Kluwer), 225

Mayor, M., & Queloz, D. 1995, *Nature*, 378, 355

Mazeh, T., Naef, D., Torres, G., Latham, D. W., Mayor, M., Beuzit, J-L., Brown, T., Buchhave, L., Burnet, M., Carney, B. W., Charbonneau, D., Drukier, G. A., Laird, J. B., Pepe, F., Perrier, C., Queloz, D., Santos, N. C., Sivan, J-P., Udry, S., & Zucker, S. 1999, submitted to *ApJ*

Sasselov, D. D., & Lester, J. B. 1994, *ApJ*, 423, 785

Seager, S. 1999, PhD Thesis, Harvard University

Seager, S., & Sasselov, D. D. 1998, *ApJ*, 502, L157

Seager, S., Whitney, B. A., & Sasselov, D. D. 1999, submitted to *ApJ*

Schneider, J. 1999, <http://cfa-www.harvard.edu/planets/>

Schneider, J. 1994, *Ap&SS*, 212, 321

Sudarsky, D., Burrows, A., & Pinto, P. 1999, submitted to *ApJ*

Smith, G. R., & Hunten, D. M. 1990, *Rev. Geophys.*, 28, 117

Tobiska, W. K. 1991, *J. Atmos. Terr. Phys.*, 53, 1005

Trilling, D. E., Brown, R. H., & Rivkin, A. S., 1999, DPS

Tsuji, T., Ohnaka, K., & Aoki, W. 1999, *ApJ*, 520, L119

Zirin, H. 1975, *ApJ*, 199, L63

Zirin, H., & Liggett, M. A. 1982, *ApJ*, 259, 719

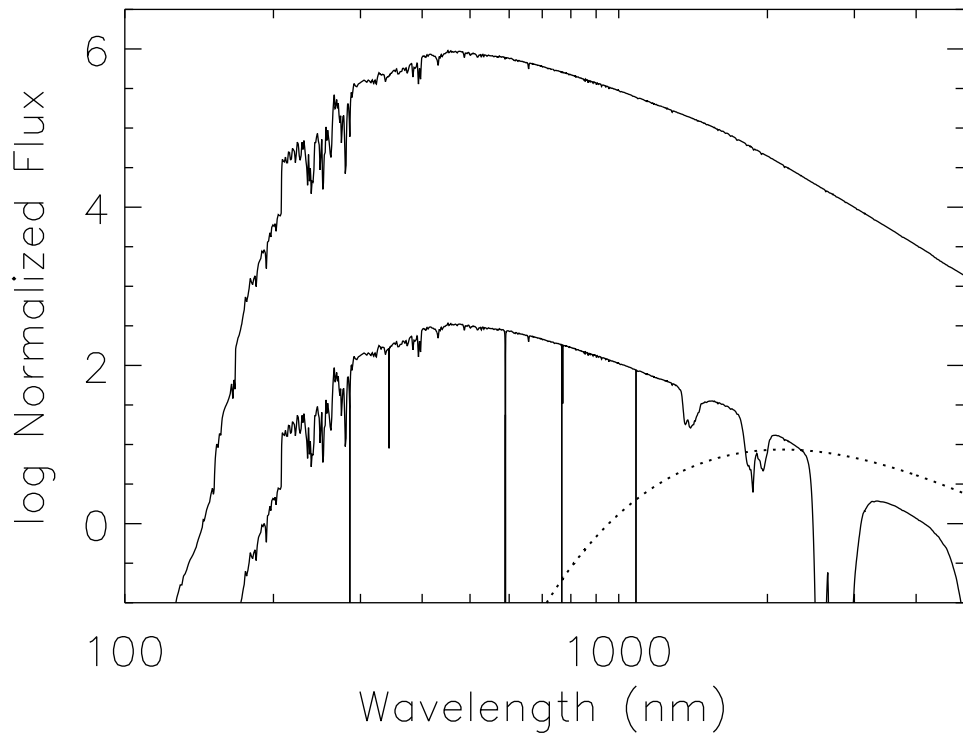


Fig. 1.— The flux of HD 209458 (upper curve) and the transmitted flux through the planet's transparent atmosphere (lower curve). Superimposed on the transmitted flux are the planetary absorption features: Na I resonance lines at 285.4 nm, 342.8 nm, and the doublet at 589.4 nm, the K I resonance doublet at 767.0 nm, and the He I triplet line at 1083 nm. The H₂O and CH₄ molecular absorption dominates in the infrared. The dotted line is a blackbody of 1350 K representative of the CEGP's thermal emission, but the thermal emission can be larger than a blackbody blueward of 2000 nm.

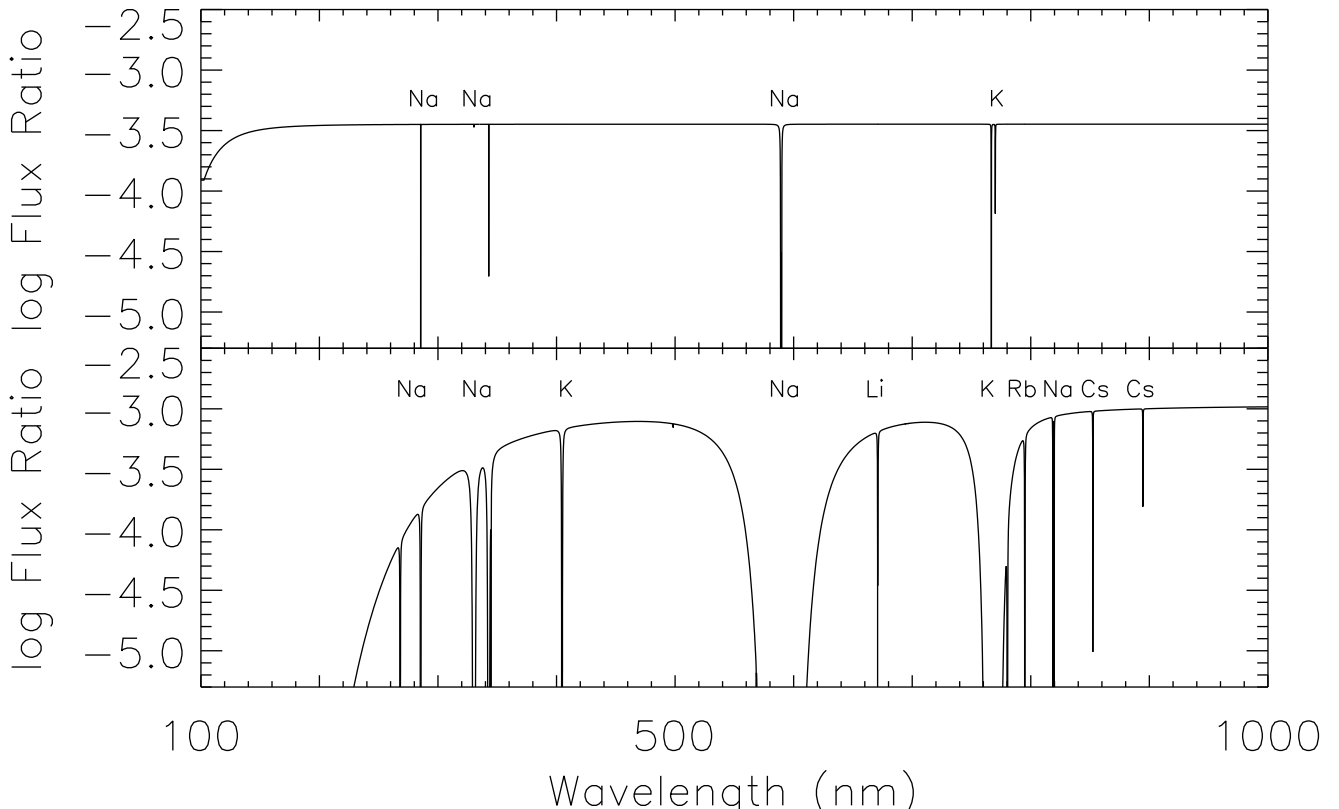


Fig. 2.— Upper plot: the ratio of the two curves in Figure 1 shows the planet absorption features (listed in Figure 1). In this model the cloud base is at 2.4×10^{-3} bar. Rayleigh scattering is important in the UV. Lower plot: a model with cloud base at 0.2 bar. The stellar flux passes through higher pressures, densities, and temperatures of the planet atmosphere compared to the model in the upper plot. In addition, a larger transparent atmosphere makes the planet-to-star flux ratio larger. Observations will constrain the cloud depth. See text for discussion.

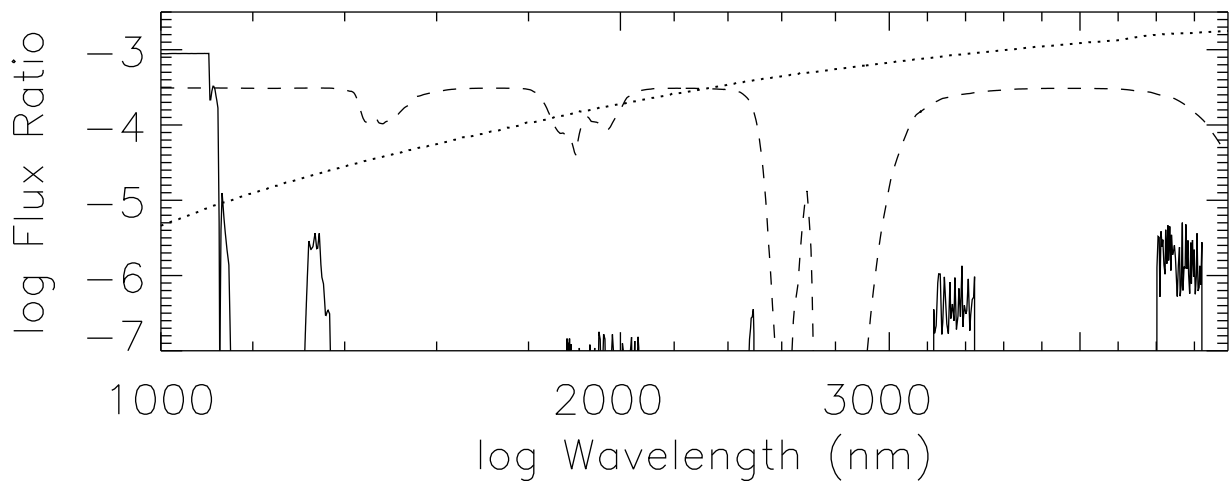


Fig. 3.— Ratio of infrared transmission spectra to the stellar spectrum for cloud base at 2.4×10^{-3} bar (dashed line) and at 0.2 bar (solid line). The dotted line is a blackbody curve of 1350 K, representative of the planet's thermal emission.